Available online at www.sciencedirect.com
ScienceDirect
Atmospheric Environment 42 (2008) 2261–2275
ATMOSPHERIC ENVIRONMENT
www.elsevier.com/locate/atmosenv

Size-differentiated source profiles for fugitive dust in the Chinese Loess Plateau

J.J. Cao[a,c,*], J.C. Chow[b,a], J.G. Watson[b,a], F. Wu[a], Y.M. Han[a], Z.D. Jin[a], Z.X. Shen[c], Z.S. An[a]

[a]State Key Laboratory of Loess and Quaternary Geology, Institute of Earth Environment, Chinese Academy of Sciences, Xi'an 710075, China
[b]Division of Atmospheric Sciences, Desert of Research Institute, Reno, USA
[c]Xi'an Jiaotong University, Xi'an, China

Received 9 August 2007; received in revised form 25 November 2007; accepted 13 December 2007

Abstract

Size-differentiated fugitive dust chemical source profiles are determined for the Chinese Loess Plateau, a major source of Asian dust. Fifteen loess samples at five sites (Yulin, Yanchi, Huanxian, Luochuan, and Xi'an) were collected, dried, sieved, resuspended, and sampled through TSP, PM_{10}, $PM_{2.5}$, and PM_1 inlets onto filters for analysis of 40 major and trace elements (Na to U), six ions (Cl^-, NO_3^-, SO_4^{2-}, Na^+, K^+, and NH_4^+), organic carbon (OC) and elemental carbon (EC), and carbonate carbon (CO_3-C). The abundances of major species ($>1\%$) include Al, Si, K, Ca, Fe, OC and CO_3-C, in four size-differentiated source profiles. OC accounted for $\sim$90% of total carbon in four size fractions for most of the profiles. Enrichment factors indicated that the 18 elements (Na, Mg, Si, K, Ca, Ti, V, Cr, Mn, Fe, Ni, Cu, Zn, Rb, Sr, Y, Zr, Ba) found in the samples were dominated by crustal sources. Enrichment factors for Co, As, Se, Mo, Cd, In, Sb, and Tl are one to two orders of magnitude larger than crustal-derived elements, suggesting the influence of anthropogenic pollution sources. Compared with loess samples, V, Cr, Ni, Cu, Zn, Sb, SO_4^{2-}, and NO_3^- are enriched in ambient $PM_{2.5}$ aerosol samples, implying that Asian dust contains pollution components in downwind regions of the desert. The elemental ratios of Si, K, Ca, Ti, Mn, and Fe to Al in Asian dust source regions compared well with those found at downwind regions such as Korea, Japan, and the North Pacific. These ratios can be used as fingerprints to trace the transport path of Asian dust.

Keywords: Size differentiation; Source profiles; Loess; Asian dust; China

1. Introduction

Large amounts of dust from Central Asia are carried by prevailing winds and deposited in East Asia, in deep-sea sediments in the remote Pacific (Duce et al., 1980), and in Greenland ice cores (Biscaye et al., 1997). China's Loess Plateau (Fig. 1) formed from the deposition of Asian dust over millions of years (Liu, 1985; An et al., 1990).

*Corresponding author at: State Key Laboratory of Loess and Quaternary Geology, Institute of Earth Environment, Chinese Academy of Sciences (CAS), No. 10 Fenghui South Road, High-Tech Zone, Xi'an 710075, China, Tel.: +86 29 8832 6488; fax: +86 29 8832 0456.
E-mail address: cao@loess.llqg.ac.cn (J.J. Cao).

1352-2310/$ - see front matter
doi:10.1016/j.atmosenv.2007.12.041

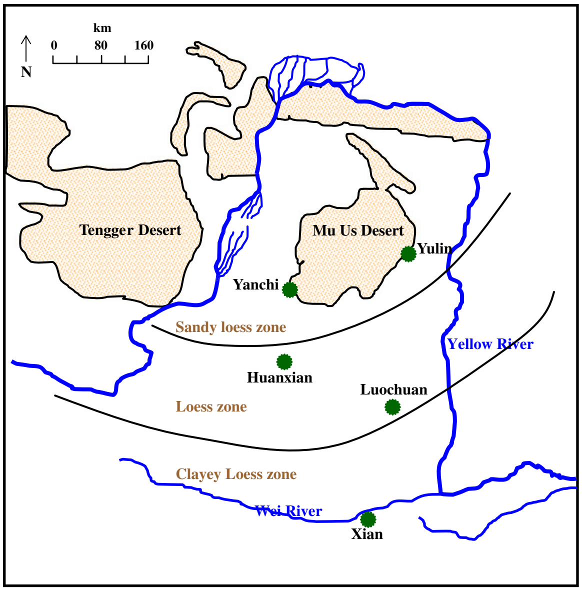

Fig. 1. Fugitive dust sampling sites (Yulin, Yanchi, Huanxian, Luochuan, Xi'an) in the Chinese Loess Plateau. The curved lines in the figure mean the boundary among sandy loess zone, loess zone, and clayey loess zone.

Nishikawa et al. (2000) and Arimoto et al. (2004) used surface soil from the Loess Plateau to represent undisturbed pre-industrial Asian dust. The Loess Plateau is arid, with much of its surface exposed, and during dry and windy weather it is a source of suspended particulate matter (PM) that pollutes cities in north China (e.g., Zhang et al., 2002; Zhao et al., 2006). Chemical source profiles are needed to quantify PM contributions from the Loess Plateau using receptor models (Watson et al., 2002; Watson and Chow, 2004, 2007).

Representative bulk surface soil sampling with resuspension and re-sampling through size-selective inlets is an effective way to obtain fugitive dust source profiles (Chow et al., 1994, 2004; Vega et al., 2001; Ashbaugh et al., 2003; Ho et al., 2003; Zhao et al., 2006; Yuan et al., 2006). This approach was applied to obtain chemical source profiles for surface soil collected at five sites on the Loess Plateau (Yulin, Yanchi, Huanxian, Luochuan, and Xi'an).

2. Methodology

2.1. Sampling sites

In China, loess occupies 440,000 km^2, including 273,000 km^2 of thick loess in the middle reaches of the Yellow River (Liu, 1985). Thick loess in the middle reaches of the Yellow River is divided into three zones (Fig. 1):

- *Sandy loess zone*: mean grain size is 0.026–0.076 mm. The coarse silt fraction (0.005–0.01 mm) is 23.6–72.4% and the clay fraction (<0.005 mm) is 7.0–20.7%.
- *Common loess zone*: mean grain size is 0.016–0.032 mm. The coarse silt fraction is 11.1–31.5% and the clay fraction is 8.1–30.4%.
- *Clayey loess zone*: mean grain size is 0.018–0.027 mm. The coarse silt fraction is 11.4–21.9% and the clay fraction is 18.0–27.8%.

Fifteen surface soil samples were collected from five sites (Yulin, Yanchi, Huanxian, Luochuan, and Xi'an) in the three loess zones as described in Table 1.

2.2. Sampling and analysis

Samples were sieved through Tyler 30, 50, 100, 200, and 400 mesh sieves to obtain about 5 g of material. The nominal geometric diameter is <38.5 μm for the 400 mesh sieve, which is equivalent to the aerodynamic diameter of TSP. Sieved samples were separated into four particle size fractions (TSP, PM_{10}, $PM_{2.5}$, and $PM_{1.0}$) and collected onto filters using the DRI resuspension systems, which was described in detail by Chow et al. (1994). Approximately 0.1 mg of sieved material was placed in a 250 ml side-arm vacuum flask sealed with a rubber stopper. Air puffs into the flask introduced dust into the chamber where a modified Parallel impactor sampling device sampled it. Clean, filtered laboratory air was drawn into the chamber by the sample flow of 10 l min^{-1} through each filter. Two kinds of filters are used, 120 filter samples were collected.

Teflon-membrane filters were equilibrated in a controlled environment (relative humidity = 25–30%, temperature = 21.5±0.5 °C) before gravimetric analysis to minimize particle volatilization and aerosol liquid water bias (Chow, 1995). Filters were weighed before and after sampling using a MT-5 microbalance (Mettler Toledo, Inc., Columbus, OH, USA) with a sensitivity of ±1 μg; the precision of re-weights for unexposed and exposed filters are below ±10 and ±15 μg, respectively. Filters were exposed to a low-level radioactive source (500 pCi of polonium210) prior to and during sample weighing

Table 1
Characteristics of field sampling sites

	Latitude	Longitude	Altitude (m)	Zone	Sample number	Land use	Surrounding environment	Population (million)
Yulin	109°78′96.4″E	38°26′06.3″N	1126	Sandy loess	3	Sandy land	Transition zone of desert and loess	0.8
Yanchi	107°58′72.7″E	37°74′90.9″N	1443	Sandy loess	3	Sandy land	Desert and salina land	0.45
Huanxian	107°31′91.4″E	36°55′32″N	1375	Loess	3	Shrub land	Farmland and village	0.35
Luochuan	109°43′60.7″E	35°75′85.6″N	1021	Loess	3	Shrub land	Farmland and village	0.2
Xi'an	108°98′37.6″E	34°20′97.6″N	416	Clayey loess	3	Cultivated land	Suburban discarded land	6.87

to remove static charge. Teflon-membrane filters were analyzed by high-sensitivity X-ray fluorescence (XRF) for Na, Mg, Al, Si, P, S, Cl, K, Ca, Ti, V, Cr, Mn, Fe, Co, Ni, Cu, Zn, Ga, As, Se, Br, Rb, Sr, Y, Zr, Mo, Pd, Ag, Cd, In, Sn, Sb, Ba, La, Au, Hg, Tl, Pb, and U (Watson et al., 1999).

Half of the quartz-fiber filters were extracted in deionized distilled water and analyzed for water-soluble chlorine (Cl^-), nitrate (NO_3^-), and sulfate (SO_4^{2-}) by ion chromatography (Chow and Watson, 1999); for water-soluble sodium (Na^+) and potassium (K^+) by atomic absorption spectrophotometry, and for water-soluble ammonium (NH_4^+) by automated colorimetry (Chow and Watson, 1998). A 0.5 cm^2 punch from the remaining half-filters was analyzed for eight carbon fractions following the IMPROVE_A thermal/optical reflectance (TOR) protocol (Chow et al., 1993, 2001, 2005, 2007). This produced four organic carbon (OC) fractions (OC1, OC2, OC3, and OC4 at 140, 280, 480, and 580 °C, respectively, in a helium atmosphere), a pyrolyzed carbon fraction (OP, determined when reflected laser light attains its original intensity after oxygen is added to the combustion atmosphere), and three elemental carbon (EC) fractions (EC1, EC2, and EC3 at 580, 740, and 840 °C, respectively, in a 98% helium/2% oxygen atmosphere). IMPROVE OC is operationally defined as OC1+OC2+OC3+OC4+OP and EC is defined as EC1+EC2+EC3−OP. The carbonate carbon (CO_3-C) abundance was determined by acidification of sample prior to thermal analysis with subsequent detection of the evolved CO_2 (Chow et al., 1993).

Resuspension of loess samples and analyses of mass, elements, ions, and carbons were conducted at the Environmental Analysis Facility (EAF) in the Division Atmosphere Sciences of the Desert Research Institute, USA. Quality assurance/quality control (QA/QC) procedures have been described in Chow et al. (1994) and Watson and Chow (2001).

3. Results and discussion

3.1. Chemical abundances

Chemical abundances for each sample were blank subtracted and calculated by dividing each chemical concentration by mass concentration, with error propagation by addition in quadrature (Watson and Chow, 2001). Tables 2–5 summarize chemical source profiles at each site in weight percent by mass for the TSP, PM_{10}, $PM_{2.5}$, and PM_1 size fractions, respectively.

3.1.1. Elemental profiles

Al, Si, K, Ca, and Fe were abundant elements with more than 1% in four size-differentiated profiles at five sites (Tables 2–5). Abundances of Si varied between 15% and 20% in TSP, 23–34% in PM_{10}, 12–15% in $PM_{2.5}$, and 12–17% in PM_1, respectively. Al contents varied around 4–6%, 7–11%, 3–6%, and 3–6%, respectively, in four size fractions. Al and Si are more abundant in PM_{10} than the other size fractions, with similar abundances found in TSP, $PM_{2.5}$, and PM_1 size fractions. According to the mineral composition of loess (Liu, 1985), quartz (SiO_2) and feldspar ($KAlSi_3O_8$) are the dominant mineral forms for Si and Al elements. The abundance of Ca varied from 4–10% in TSP, to 6–17% in PM_{10}, $PM_{2.5}$, and PM_1 fractions. Calcite ($CaCO_3$) is also a dominant mineral found in loess, but it is the most active mineral in loess because

Table 2
Summary of fugitive dust source profiles (weight percent by mass) for TSP in Chinese Loess plateau

Species	Yulin	Yanchi	Huanxian	Luochuan	Xi'an	Composite	Loess (Wen, 1989)
Na	0.0705±0.5395[a]	0.1373±0.5524	0.3130±0.4527	0.1502±0.3396	0.1477±0.3151	0.1637	1.26 (0.77–1.72)
Mg	0.1026±0.1119	0.1890±0.0843	0.1263±0.0850	0.2311±0.0267	0.1851±0.0243	0.1668	2.07 (0.49–10.28)
Al	6.3397±1.2422	4.3928±0.7715	4.5516±0.7964	6.2484±1.0768	6.3636±1.1090	5.5792	6.06 (4.11–7.83)
Si	20.1247±4.1732	15.1426±2.8154	15.5903±2.9103	17.9434±3.2873	18.9113±3.4858	17.5425	25.55 (22.19–29.71)
P	0.0319±0.0136	0.0390±0.0118	0.0197±0.0155	0.0176±0.0120	0.0559±0.0149	0.0328	0.0462(0.0131–0.135)
S	0.0174±0.0032	0.0230±0.0027	0.0289±0.0021	0.0269±0.0017	0.0514±0.0022	0.0295	
Cl	0.0678±0.0145	0.0550±0.0111	0.0386±0.0076	0.0453±0.0086	0.0868±0.0160	0.0587	
K	1.6981±0.2133	1.4341±0.1703	1.5713±0.1835	1.8613±0.2163	2.0351±0.2376	1.72	1.63 (0.17–2.31)
Ca	6.1010±0.7467	10.2251±1.0289	7.0989±0.7163	4.4302±0.4421	6.0392±0.5982	6.7789	5.63 (1.35–9.24)
Ti	0.3163±0.0310	0.2582±0.0203	0.2603±0.0101	0.3371±0.0113	0.3180±0.0105	0.298	0.366(0.1679–0.4676)
V	0.0077±0.0189	0.0103±0.0110	0.0112±0.0070	0.0133±0.0052	0.0113±0.0059	0.0107	0.009(0.003–0.01)
Cr	0.0058±0.0051	0.0062±0.0028	0.0068±0.0007	0.0082±0.0009	0.0083±0.0008	0.0071	0.008(0.002–0.01)
Mn	0.0682±0.0036	0.0596±0.0026	0.0632±0.0022	0.0825±0.0028	0.0879±0.0029	0.0723	0.0634(0.031–0.0878)
Fe	3.0223±0.1249	2.5407±0.0905	2.7079±0.0884	3.7396±0.1167	3.5977±0.1107	3.1216	3.88 (1.62–6.29)
Co	0.0065±0.0284	0.0038±0.0230	0.0051±0.0242	0.0088±0.0338	0.0058±0.0323	0.006	0.0021(0.0014–0.0028)
Ni	0.0035±0.0011	0.0030±0.0007	0.0021±0.0002	0.0036±0.0003	0.0036±0.0002	0.0032	0.0021(0.0014–0.0028)
Cu	0.0030±0.0011	0.0025±0.0007	0.0027±0.0002	0.0032±0.0002	0.0040±0.0002	0.0031	0.0025(0.0013–0.0035)
Zn	0.0124±0.0012	0.0101±0.0008	0.0067±0.0003	0.0088±0.0003	0.0104±0.0004	0.0097	0.0079(0.0039–0.0147)
Ga	0.0000±0.0031	0.0000±0.0024	0.0000±0.0018	0.0002±0.0013	0.0000±0.0009	0.0000	0.001(0.0003–0.002)
As	0.0017±0.0030	0.0010±0.0023	0.0012±0.0016	0.0016±0.0011	0.0017±0.0006	0.0015	0.001(0–0.002)
Se	0.0005±0.0015	0.0000±0.0011	0.0002±0.0007	0.0003±0.0005	0.0002±0.0004	0.0002	0.0000051
Br	0.0001±0.0012	0.0006±0.0009	0.0003±0.0006	0.0002±0.0004	0.0003±0.0004	0.0003	
Rb	0.0072±0.0011	0.0066±0.0007	0.0068±0.0004	0.0091±0.0004	0.0100±0.0003	0.0079	
Sr	0.0144±0.0014	0.0194±0.0011	0.0214±0.0008	0.0124±0.0005	0.0153±0.0005	0.0166	0.0195(0.0152–0.0288)
Y	0.0027±0.0015	0.0018±0.0013	0.0018±0.0007	0.0029±0.0006	0.0027±0.0003	0.0024	
Zr	0.0094±0.0018	0.0083±0.0012	0.0082±0.0005	0.0080±0.0004	0.0092±0.0004	0.0086	0.025(0.007–0.05)
Mo	0.0020±0.0036	0.0011±0.0026	0.0012±0.0016	0.0000±0.0012	0.0007±0.0009	0.001	0.000059
Pd	0.0012±0.0095	0.0009±0.0062	0.0002±0.0022	0.0002±0.0017	0.0002±0.0013	0.0005	
Ag	0.0012±0.0115	0.0016±0.0076	0.0003±0.0027	0.0005±0.0020	0.0007±0.0016	0.0008	
Cd	0.0023±0.0121	0.0008±0.0079	0.0023±0.0026	0.0019±0.0019	0.0010±0.0016	0.0016	
In	0.0018±0.0136	0.0018±0.0090	0.0013±0.0034	0.0004±0.0024	0.0010±0.0019	0.0012	
Sn	0.0020±0.0181	0.0024±0.0120	0.0025±0.0050	0.0021±0.0037	0.0007±0.0028	0.002	
Sb	0.0005±0.0203	0.0000±0.0135	0.0013±0.0059	0.0003±0.0042	0.0000±0.0033	0.0004	
Ba	0.0099±0.0758	0.0175±0.0519	0.0200±0.0269	0.0352±0.0195	0.0371±0.0120	0.0239	0.0579(0.05–0.0647)
La	0.0000±0.0995	0.0141±0.0680	0.0040±0.0344	0.0057±0.0252	0.0080±0.0186	0.0064	
Au	0.0000±0.0041	0.0003±0.0030	0.0003±0.0019	0.0000±0.0014	0.0011±0.0010	0.0003	
Hg	0.0005±0.0030	0.0009±0.0021	0.0006±0.0012	0.0005±0.0009	0.0008±0.0006	0.0006	
Tl	0.0006±0.0029	0.0011±0.0020	0.0003±0.0011	0.0002±0.0008	0.0001±0.0006	0.0005	
Pb	0.0058±0.0034	0.0046±0.0026	0.0044±0.0013	0.0032±0.0012	0.0044±0.0004	0.0045	0.003(0.0015–0.004)
U	0.0011±0.0034	0.0001±0.0026	0.0001±0.0018	0.0003±0.0015	0.0002±0.0013	0.0004	
Cl^-	0.1059±0.0376	0.1740±0.0308	0.1578±0.0226	0.0791±0.0138	0.1726±0.019	0.1379	
NO_3^-	0.0000±0.0342	0.0000±0.0240	0.0000±0.0165	0.0000±0.0119	0.0000±0.0116	0.0000	
SO_4^{2-}	0.0000±0.0342	0.0000±0.0240	0.0168±0.0166	0.0415±0.0121	0.1473±0.0128	0.0411	
NH_4^+	0.0602±0.0344	0.0616±0.0242	0.0372±0.0166	0.0394±0.0120	0.0617±0.0120	0.052	
Na^+	0.0295±0.0266	0.0367±0.0168	0.0587±0.0032	0.0248±0.0021	0.0401±0.0032	0.038	
K^+	0.0630±0.0268	0.0793±0.0172	0.0838±0.0043	0.0576±0.0031	0.1653±0.0092	0.0898	
OC1	0.0000±0.1833	0.0104±0.1157	0.0066±0.0160	0.0011±0.0149	0.0096±0.0193	0.0055	
OC2	0.0444±0.1867	0.0858±0.1190	0.1915±0.0303	0.2527±0.0270	0.1621±0.0263	0.1473	
OC3	0.3799±0.2353	0.4355±0.1623	0.4336±0.0984	0.5173±0.0828	0.6749±0.0914	0.4883	
OC4	0.2269±0.1902	0.2672±0.1250	0.3091±0.0485	0.2994±0.0393	0.4766±0.0503	0.3158	
OP	0.4568±0.1994	0.4540±0.1382	0.3900±0.0729	0.5200±0.0813	0.5931±0.0989	0.4828	
OC	1.1080±0.4480	1.2529±0.2994	1.3309±0.1406	1.5904±0.1310	1.9163±0.1516	1.4397	
EC1	0.3184±0.0775	0.3293±0.0702	0.2093±0.0478	0.3303±0.0590	0.4630±0.0800	0.33	
EC2	0.1293±0.0552	0.1328±0.0381	0.1176±0.0234	0.1494±0.0174	0.1571±0.0175	0.1372	
EC3	0.0094±0.0448	0.0338±0.0309	0.0635±0.0235	0.0402±0.0163	0.0282±0.0138	0.035	
EC	0.0003±0.2245	0.0419±0.1614	0.0004±0.0920	0.0000±0.1020	0.0553±0.1278	0.0196	
TC	1.1083±0.5011	1.2948±0.3404	1.3313±0.1681	1.5903±0.1660	1.9716±0.1984	1.4592	
CO_3-C	1.5032±0.1062	2.1416±0.1248	2.4643±0.1343	1.0869±0.0572	1.6764±0.0911	1.7745	

[a]The value is the average and analytic uncertainty of three samples at each site.

Table 3
Summary of fugitive dust source profiles (weight percent by mass) for PM_{10} in Chinese Loess Plateau

Species	Yulin	Yanchi	Huanxian	Luochuan	Xi'an	Composite
Na	1.6263±0.6754	0.0819±0.8884	0.3070±0.6444	0.0356±0.4441	0.0663±0.4947	0.4234
Mg	0.4726±0.1469	0.4096±0.1372	0.4926±0.0492	0.2060±0.0902	0.1790±0.0868	0.3520
Al	11.0262±2.0930	6.9416±1.2101	8.4686±1.4593	9.8325±1.7006	9.4093±1.6270	9.1356
Si	34.1999±6.8344	23.3983±4.3386	24.9884±4.5776	27.5435±5.0606	26.9415±4.9527	27.4143
P	0.0609±0.0252	0.0368±0.0246	0.0743±0.0204	0.0245±0.0180	0.0581±0.0158	0.0509
S	0.0508±0.0065	0.0375±0.0049	0.0513±0.0031	0.0426±0.0024	0.0722±0.0032	0.0509
Cl	0.0872±0.0207	0.0837±0.0192	0.0566±0.0114	0.0583±0.0104	0.0924±0.0161	0.0757
K	2.5927±0.3279	2.0043±0.2359	2.4749±0.2857	2.7475±0.3178	2.7724±0.3200	2.5184
Ca	8.7928±1.0156	15.0331±1.5184	10.7256±1.0630	6.3566±0.6433	8.2579±0.8114	9.8332
Ti	0.4861±0.0568	0.3324±0.0387	0.3651±0.0137	0.4647±0.0164	0.4010±0.0138	0.4099
V	0.0182±0.0346	0.0119±0.0228	0.0139±0.0118	0.0207±0.0044	0.0160±0.0062	0.0161
Cr	0.0113±0.0091	0.0069±0.0052	0.0073±0.0012	0.0123±0.0014	0.0097±0.0012	0.0095
Mn	0.1116±0.0064	0.0841±0.0039	0.0935±0.0031	0.1199±0.0040	0.1208±0.0039	0.1060
Fe	4.5304±0.1969	3.3336±0.1165	4.0511±0.1248	5.3037±0.1673	4.7585±0.1470	4.3955
Co	0.0103±0.0432	0.0069±0.0302	0.0090±0.0361	0.0101±0.0473	0.0066±0.0423	0.0086
Ni	0.0060±0.0020	0.0041±0.0014	0.0041±0.0003	0.0051±0.0004	0.0047±0.0003	0.0048
Cu	0.0062±0.0021	0.0051±0.0015	0.0043±0.0004	0.0046±0.0004	0.0047±0.0003	0.0050
Zn	0.0291±0.0025	0.0157±0.0015	0.0113±0.0005	0.0128±0.0005	0.0125±0.0005	0.0163
Ga	0.0000±0.0060	0.0003±0.0044	0.0000±0.0024	0.0000±0.0015	0.0000±0.0016	0.0001
As	0.0041±0.0056	0.0030±0.0041	0.0029±0.0020	0.0020±0.0014	0.0019±0.0015	0.0028
Se	0.0000±0.0028	0.0000±0.0020	0.0001±0.0009	0.0003±0.0006	0.0005±0.0006	0.0002
Br	0.0001±0.0023	0.0005±0.0018	0.0002±0.0008	0.0001±0.0006	0.0003±0.0006	0.0002
Rb	0.0095±0.0021	0.0078±0.0015	0.0100±0.0005	0.0133±0.0005	0.0135±0.0005	0.0108
Sr	0.0186±0.0024	0.0297±0.0019	0.0317±0.0011	0.0179±0.0007	0.0181±0.0007	0.0232
Y	0.0021±0.0035	0.0051±0.0019	0.0029±0.0008	0.0060±0.0005	0.0034±0.0004	0.0039
Zr	0.0127±0.0032	0.0083±0.0023	0.0112±0.0007	0.0121±0.0006	0.0115±0.0006	0.0112
Mo	0.0022±0.0068	0.0029±0.0048	0.0000±0.0024	0.0005±0.0015	0.0002±0.0015	0.0012
Pd	0.0031±0.0179	0.0002±0.0126	0.0008±0.0030	0.0008±0.0025	0.0009±0.0021	0.0011
Ag	0.0000±0.0217	0.0029±0.0154	0.0016±0.0039	0.0006±0.0032	0.0004±0.0027	0.0011
Cd	0.0024±0.0227	0.0048±0.0161	0.0019±0.0038	0.0005±0.0033	0.0003±0.0026	0.0020
In	0.0035±0.0257	0.0036±0.0182	0.0004±0.0047	0.0018±0.0038	0.0024±0.0032	0.0023
Sn	0.0018±0.0340	0.0010±0.0242	0.0000±0.0068	0.0008±0.0054	0.0024±0.0045	0.0012
Sb	0.0000±0.0382	0.0000±0.0273	0.0001±0.0082	0.0000±0.0062	0.0024±0.0056	0.0005
Ba	0.0158±0.1434	0.0264±0.1029	0.0341±0.0370	0.0262±0.0247	0.0464±0.0200	0.0298
La	0.0376±0.1889	0.0192±0.1347	0.0126±0.0469	0.0047±0.0337	0.0081±0.0317	0.0164
Au	0.0000±0.0079	0.0000±0.0057	0.0000±0.0027	0.0004±0.0017	0.0000±0.0018	0.0001
Hg	0.0010±0.0057	0.0014±0.0041	0.0004±0.0016	0.0010±0.0011	0.0010±0.0011	0.0010
Tl	0.0000±0.0054	0.0004±0.0039	0.0019±0.0014	0.0006±0.0011	0.0011±0.0010	0.0008
Pb	0.0099±0.0065	0.0077±0.0046	0.0034±0.0029	0.0070±0.0009	0.0063±0.0008	0.0069
U	0.0000±0.0063	0.0012±0.0046	0.0004±0.0026	0.0002±0.0019	0.0000±0.0020	0.0004
Cl^-	0.3233±0.0889	0.2763±0.0678	0.2318±0.0329	0.1673±0.0247	0.2833±0.0335	0.2564
NO_3^-	0.0000±0.0807	0.0000±0.0596	0.0000±0.0257	0.0000±0.0189	0.0000±0.0185	0.0000
SO_4^{2-}	0.0000±0.0807	0.0000±0.0596	0.0286±0.0257	0.0442±0.0190	0.2096±0.0198	0.0565
NH_4^+	0.1861±0.0813	0.1629±0.0601	0.0888±0.0260	0.0806±0.0193	0.0856±0.0189	0.1208
Na^+	0.0828±0.0619	0.0662±0.0436	0.1003±0.0064	0.0383±0.0071	0.0605±0.0051	0.0696
K^+	0.1677±0.0624	0.1602±0.0442	0.1559±0.0083	0.1089±0.0085	0.1571±0.0078	0.1499
OC1	0.0152±0.4265	0.0083±0.3005	0.0462±0.0348	0.0421±0.0491	0.0076±0.0301	0.0239
OC2	0.2243±0.4351	0.4087±0.3083	0.4639±0.0561	0.2722±0.0577	0.2938±0.0422	0.3326
OC3	0.8031±0.5450	1.4130±0.4184	1.0008±0.1703	0.5310±0.1212	0.9409±0.1335	0.9378
OC4	0.6131±0.4440	1.4687±0.3425	0.6312±0.0850	0.3103±0.0655	0.6275±0.0697	0.7301
OP	0.9620±0.4560	2.3728±0.4714	0.7249±0.1201	0.3483±0.0729	1.1337±0.1524	1.1083
OC	2.6177±1.0383	5.6715±0.8465	2.8671±0.2425	1.5040±0.1762	3.0034±0.2274	3.1327
EC1	0.7197±0.1759	1.5509±0.2737	0.4936±0.0967	0.2431±0.0466	0.7574±0.1180	0.7530
EC2	0.2559±0.1292	0.6869±0.0993	0.2231±0.0365	0.0978±0.0272	0.2819±0.0273	0.3091
EC3	0.0116±0.1040	0.1823±0.0991	0.0673±0.0231	0.0073±0.0140	0.0945±0.0303	0.0726
EC	0.0252±0.5143	0.0472±0.5547	0.0591±0.1584	0.0000±0.0911	0.0001±0.1946	0.0263
TC	2.6428±1.1587	5.7187±1.0121	2.9262±0.2901	1.5040±0.1984	3.0035±0.2993	3.1590
CO_3-C	4.1051±0.2995	5.7127±0.3099	3.2829±0.1648	1.6250±0.0878	2.1529±0.1114	3.3757

Table 4
Summary of fugitive dust source profiles (weight percent by mass) for $PM_{2.5}$ in Chinese Loess Plateau

Species	Yulin	Yanchi	Huanxian	Luochuan	Xi'an	Composite
Na	0.0000 ± 3.5714	0.8568 ± 2.6914	0.0000 ± 0.6030	0.0000 ± 0.6147	0.0463 ± 0.4403	0.1806
Mg	0.3006 ± 0.7466	0.5970 ± 0.5405	0.5143 ± 0.0520	0.3521 ± 0.0514	0.2840 ± 0.0371	0.4096
Al	3.7145 ± 0.5580	3.6884 ± 0.2480	4.4767 ± 0.1874	5.7933 ± 0.2445	4.6522 ± 0.1923	4.4650
Si	11.6802 ± 1.5750	12.4751 ± 0.7333	12.9962 ± 0.5341	14.8248 ± 0.6166	12.7633 ± 0.5219	12.9479
P	0.0180 ± 0.0347	0.0462 ± 0.0220	0.0233 ± 0.0084	0.0284 ± 0.0084	0.0573 ± 0.0045	0.0346
S	0.0242 ± 0.0535	0.0336 ± 0.0406	0.0584 ± 0.0038	0.0547 ± 0.0039	0.0693 ± 0.0037	0.0480
Cl	0.0622 ± 0.0955	0.0937 ± 0.0620	0.0614 ± 0.0059	0.0477 ± 0.0063	0.0568 ± 0.0045	0.0644
K	1.5826 ± 0.1958	1.9703 ± 0.1227	2.3458 ± 0.0968	2.3700 ± 0.0986	2.3266 ± 0.0954	2.1191
Ca	14.2412 ± 1.1793	17.4827 ± 1.1656	10.1138 ± 0.4240	7.2709 ± 0.3356	6.7986 ± 0.2836	11.1814
Ti	0.2938 ± 0.3078	0.2609 ± 0.2407	0.3684 ± 0.0247	0.4387 ± 0.0287	0.3987 ± 0.0212	0.3521
V	0.0011 ± 0.1642	0.0119 ± 0.1240	0.0169 ± 0.0125	0.0186 ± 0.0133	0.0181 ± 0.0084	0.0133
Cr	0.0087 ± 0.0392	0.0072 ± 0.0333	0.0101 ± 0.0026	0.0152 ± 0.0030	0.0130 ± 0.0020	0.0108
Mn	0.0545 ± 0.0227	0.1152 ± 0.0138	0.1057 ± 0.0047	0.1250 ± 0.0056	0.1487 ± 0.0063	0.1098
Fe	3.7747 ± 0.4080	3.8679 ± 0.2177	4.6535 ± 0.1910	5.8498 ± 0.2426	5.2128 ± 0.2130	4.6717
Co	0.0091 ± 0.0577	0.0062 ± 0.0390	0.0051 ± 0.0417	0.0102 ± 0.0527	0.0120 ± 0.0464	0.0085
Ni	0.0045 ± 0.0123	0.0067 ± 0.0081	0.0050 ± 0.0008	0.0057 ± 0.0009	0.0051 ± 0.0006	0.0054
Cu	0.0050 ± 0.0121	0.0073 ± 0.0090	0.0048 ± 0.0008	0.0049 ± 0.0009	0.0054 ± 0.0006	0.0055
Zn	0.0120 ± 0.0113	0.0193 ± 0.0071	0.0131 ± 0.0009	0.0143 ± 0.0010	0.0138 ± 0.0008	0.0145
Ga	0.0000 ± 0.0330	0.0000 ± 0.0212	0.0008 ± 0.0022	0.0012 ± 0.0026	0.0004 ± 0.0016	0.0005
As	0.0014 ± 0.0330	0.0142 ± 0.0200	0.0026 ± 0.0021	0.0036 ± 0.0018	0.0020 ± 0.0016	0.0048
Se	0.0002 ± 0.0157	0.0003 ± 0.0099	0.0004 ± 0.0010	0.0000 ± 0.0012	0.0000 ± 0.0007	0.0002
Br	0.0002 ± 0.0140	0.0005 ± 0.0091	0.0000 ± 0.0010	0.0006 ± 0.0011	0.0003 ± 0.0007	0.0003
Rb	0.0086 ± 0.0148	0.0055 ± 0.0094	0.0126 ± 0.0009	0.0144 ± 0.0011	0.0140 ± 0.0008	0.0110
Sr	0.0180 ± 0.0134	0.0387 ± 0.0087	0.0378 ± 0.0018	0.0188 ± 0.0013	0.0178 ± 0.0009	0.0262
Y	0.0034 ± 0.0199	0.0080 ± 0.0131	0.0035 ± 0.0010	0.0073 ± 0.0012	0.0029 ± 0.0007	0.0050
Zr	0.0086 ± 0.0196	0.0062 ± 0.0150	0.0103 ± 0.0013	0.0122 ± 0.0015	0.0105 ± 0.0009	0.0096
Mo	0.0011 ± 0.0381	0.0124 ± 0.0247	0.0000 ± 0.0025	0.0006 ± 0.0030	0.0006 ± 0.0018	0.0029
Pd	0.0003 ± 0.1037	0.0003 ± 0.0659	0.0011 ± 0.0066	0.0007 ± 0.0075	0.0003 ± 0.0046	0.0005
Ag	0.0000 ± 0.1258	0.0024 ± 0.0807	0.0015 ± 0.0081	0.0015 ± 0.0092	0.0004 ± 0.0056	0.0012
Cd	0.0008 ± 0.1325	0.0013 ± 0.0842	0.0018 ± 0.0085	0.0005 ± 0.0096	0.0005 ± 0.0059	0.0010
In	0.0028 ± 0.1495	0.0023 ± 0.0951	0.0009 ± 0.0096	0.0013 ± 0.0109	0.0000 ± 0.0066	0.0015
Sn	0.0049 ± 0.1989	0.0053 ± 0.1258	0.0019 ± 0.0127	0.0031 ± 0.0145	0.0004 ± 0.0088	0.0031
Sb	0.0000 ± 0.2224	0.0013 ± 0.1412	0.0008 ± 0.0143	0.0006 ± 0.0163	0.0000 ± 0.0099	0.0005
Ba	0.0561 ± 0.8249	0.2055 ± 0.5276	0.0424 ± 0.0512	0.0646 ± 0.0534	0.0481 ± 0.0341	0.0833
La	0.0310 ± 1.0867	0.2275 ± 0.6919	0.0140 ± 0.0699	0.0024 ± 0.0806	0.0048 ± 0.0487	0.0559
Au	0.0038 ± 0.0436	0.0000 ± 0.0282	0.0002 ± 0.0029	0.0017 ± 0.0034	0.0007 ± 0.0021	0.0013
Hg	0.0003 ± 0.0327	0.0075 ± 0.0211	0.0016 ± 0.0022	0.0002 ± 0.0025	0.0007 ± 0.0015	0.0021
Tl	0.0005 ± 0.0307	0.0001 ± 0.0195	0.0001 ± 0.0020	0.0015 ± 0.0023	0.0005 ± 0.0014	0.0005
Pb	0.0061 ± 0.0375	0.0097 ± 0.0290	0.0071 ± 0.0023	0.0059 ± 0.0033	0.0085 ± 0.0017	0.0075
U	0.0000 ± 0.0348	0.0000 ± 0.0224	0.0003 ± 0.0027	0.0001 ± 0.0031	0.0001 ± 0.0021	0.0001
Cl^-	0.1120 ± 0.4357	0.2891 ± 0.2343	0.1319 ± 0.0273	0.0992 ± 0.0292	0.1669 ± 0.0235	0.1598
NO_3^-	0.0000 ± 0.3635	0.0000 ± 0.2234	0.0000 ± 0.0230	0.0000 ± 0.0260	0.0232 ± 0.0150	0.0046
SO_4^{2-}	0.0000 ± 0.3635	0.0000 ± 0.2234	0.0976 ± 0.0233	0.0404 ± 0.0262	0.0781 ± 0.0165	0.0432
NH_4^+	0.1145 ± 0.3706	0.1857 ± 0.2239	0.0520 ± 0.0232	0.1007 ± 0.0265	0.0790 ± 0.0164	0.1064
Na^+	0.0305 ± 0.2871	0.1184 ± 0.1753	0.1169 ± 0.0191	0.0408 ± 0.0205	0.0479 ± 0.0127	0.0709
K^+	0.1145 ± 0.2911	0.2945 ± 0.1770	0.3322 ± 0.0253	0.1920 ± 0.0225	0.2124 ± 0.0163	0.2291
OC1	0.0000 ± 1.9659	0.0803 ± 1.2076	0.0768 ± 0.1245	0.0000 ± 0.1406	0.0000 ± 0.0859	0.0314
OC2	0.0000 ± 2.0139	0.6533 ± 1.2312	0.0972 ± 0.1269	0.0000 ± 0.1430	0.0047 ± 0.0875	0.1510
OC3	0.0821 ± 2.5729	2.0682 ± 1.5433	0.1934 ± 0.1566	0.4510 ± 0.1864	0.3466 ± 0.1161	0.6283
OC4	0.0821 ± 2.0663	1.8271 ± 1.2633	0.3413 ± 0.1315	0.3296 ± 0.1489	0.2581 ± 0.0918	0.5676
OP	0.0000 ± 2.0135	1.0141 ± 1.2313	0.4114 ± 0.1382	0.6724 ± 0.1740	0.3846 ± 0.1025	0.4965
OC	0.1642 ± 4.8581	5.6430 ± 2.9244	1.1201 ± 0.3057	1.4530 ± 0.3592	0.9941 ± 0.2193	1.8749
EC1	0.0870 ± 1.0570	1.3489 ± 0.4140	0.2651 ± 0.0563	0.4630 ± 0.0905	0.2736 ± 0.0513	0.4875
EC2	0.0000 ± 0.6017	0.1728 ± 0.3584	0.1212 ± 0.0372	0.1738 ± 0.0424	0.1014 ± 0.0258	0.1138
EC3	0.0000 ± 0.4778	0.0094 ± 0.2935	0.0255 ± 0.0318	0.0356 ± 0.0361	0.0097 ± 0.0212	0.0160
EC	0.0870 ± 2.3863	0.5172 ± 1.3771	0.0004 ± 0.1563	0.0000 ± 0.2020	0.0001 ± 0.1185	0.1209
TC	0.2512 ± 5.4882	6.1602 ± 3.2384	1.1205 ± 0.3433	1.4530 ± 0.4121	0.9942 ± 0.2493	1.9958
CO_3-C	4.0761 ± 0.4965	4.6785 ± 0.4275	3.7196 ± 0.2172	1.1413 ± 0.0736	0.9121 ± 0.0570	2.9055

Table 5
Summary of fugitive dust source profiles (weight percent by mass) for PM_1 in Chinese Loess Plateau

Species	Yulin	Yanchi	Huanxian	Luochuan	Xi'an	Composite
Na	0.0000±6.6556	1.7104±1.1822	0.4740±0.7390	0.6570±0.9338	0.5245±0.5820	0.6732
Mg	0.1474±1.2436	0.4562±0.2193	0.4586±0.0592	0.4359±0.0775	0.6086±0.0600	0.4213
Al	4.8582±0.7104	3.6529±0.2019	4.2157±0.1811	6.3803±0.2755	5.4114±0.2277	4.9037
Si	14.6001±1.8738	12.8498±0.6628	12.2708±0.5099	16.8320±0.7083	14.7756±0.6085	14.2657
P	0.2129±0.0699	0.0725±0.0109	0.0188±0.0117	0.0162±0.0124	0.0600±0.0061	0.0761
S	0.0107±0.1116	0.0612±0.0084	0.0444±0.0062	0.0510±0.0059	0.0842±0.0051	0.0503
Cl	0.1151±0.1702	0.0815±0.0171	0.0617±0.0078	0.0577±0.0110	0.0586±0.0072	0.0749
K	1.7237±0.2205	1.8823±0.0991	2.1751±0.0907	2.5712v0.1080	2.4954±0.1032	2.1695
Ca	8.6535±2.0640	16.3937±0.8715	10.1487±0.4363	7.0877±0.3487	7.6682±0.3282	9.9904
Ti	0.4211±0.6666	0.3552±0.0667	0.3474±0.0314	0.4677±0.0468	0.3987±0.0298	0.398
V	0.0206±0.2997	0.0145±0.0391	0.0142±0.0174	0.0217±0.0270	0.0179±0.0150	0.0178
Cr	0.0165±0.0716	0.0102±0.0097	0.0102±0.0036	0.0111±0.0054	0.0120±0.0033	0.012
Mn	0.0973±0.0359	0.1068±0.0070	0.1040±0.0048	0.1424±0.0068	0.1556±0.0068	0.1212
Fe	3.9320±0.4354	3.7451±0.1921	4.3942±0.1822	6.1198±0.2550	5.4068±0.2224	4.7196
Co	0.0038±0.0591	0.0056±0.0422	0.0135±0.0398	0.0067±0.0553	0.0081±0.0485	0.0075
Ni	0.0082±0.0234	0.0037±0.0024	0.0050±0.0011	0.0056±0.0016	0.0052±0.0010	0.0056
Cu	0.0063±0.0260	0.0077±0.0026	0.0048±0.0011	0.0045±0.0020	0.0056±0.0010	0.0058
Zn	0.0182±0.0253	0.0144±0.0025	0.0127±0.0012	0.0163±0.0017	0.0166±0.0012	0.0156
Ga	0.0355±0.0622	0.0000±0.0073	0.0012±0.0033	0.0004±0.0051	0.0000±0.0029	0.0074
As	0.0334±0.0587	0.0036±0.0070	0.0029±0.0030	0.0055±0.0048	0.0027±0.0030	0.0096
Se	0.0042±0.0294	0.0000±0.0034	0.0001±0.0015	0.0004±0.0024	0.0000±0.0014	0.0009
Br	0.0000±0.0245	0.0005±0.0030	0.0000±0.0013	0.0006±0.0021	0.0005±0.0012	0.0003
Rb	0.0037±0.0277	0.0086±0.0025	0.0105±0.0012	0.0163±0.0018	0.0154±0.0012	0.0109
Sr	0.0185±0.0313	0.0322±0.0033	0.0325±0.0019	0.0190±0.0020	0.0206±0.0014	0.0246
Y	0.0044±0.0388	0.0022±0.0045	0.0033±0.0015	0.0046±0.0030	0.0029±0.0016	0.0035
Zr	0.0043±0.0447	0.0104±0.0040	0.0096±0.0018	0.0121±0.0027	0.0097±0.0016	0.0092
Mo	0.0000±0.0722	0.0042±0.0084	0.0000±0.0037	0.0004±0.0059	0.0009±0.0034	0.0011
Pd	0.0000±0.1864	0.0015±0.0220	0.0005±0.0095	0.0006±0.0145	0.0011±0.0086	0.0007
Ag	0.0152±0.2276	0.0037±0.0266	0.0006±0.0115	0.0040±0.0177	0.0001±0.0104	0.0047
Cd	0.0599±0.2373	0.0077±0.0281	0.0017±0.0121	0.0031±0.0185	0.0020±0.0108	0.0149
In	0.0000±0.2688	0.0101±0.0318	0.0034±0.0138	0.0036±0.0210	0.0013±0.0123	0.0037
Sn	0.0038±0.3558	0.0057±0.0420	0.0031±0.0183	0.0028±0.0278	0.0000±0.0163	0.0031
Sb	0.0000±0.3979	0.0000±0.0473	0.0000±0.0206	0.0016±0.0315	0.0000±0.0184	0.0003
Ba	0.0125±1.4996	0.0000±0.1763	0.0301±0.0771	0.0465±0.1166	0.0557±0.0689	0.029
La	0.0272±1.9733	0.0390±0.2324	0.0137±0.1013	0.0388±0.1563	0.0003±0.0904	0.0238
Au	0.0240±0.0813	0.0000±0.0096	0.0012±0.0043	0.0011±0.0066	0.0000±0.0038	0.0053
Hg	0.0072±0.0603	0.0018±0.0071	0.0010±0.0031	0.0007±0.0048	0.0003±0.0028	0.0022
Tl	0.0039±0.0560	0.0004±0.0066	0.0014±0.0029	0.0044±0.0039	0.0010±0.0026	0.0022
Pb	0.0064±0.0852	0.0072±0.0101	0.0066±0.0043	0.0027±0.0072	0.0098±0.0036	0.0065
U	0.0064±0.0669	0.0011±0.0079	0.0017±0.0036	0.0000±0.0059	0.0005±0.0035	0.0019
Cl^-	1.8103±0.8846	0.2542±0.0963	0.1437±0.0420	0.1758±0.0626	0.1043±0.0367	0.4977
NO_3^-	0.0000±0.7419	0.0000±0.0874	0.0000±0.0378	0.0000±0.0574	0.0000±0.0338	0.0000
SO_4^{2-}	0.0000±0.7419	0.0000±0.0874	0.0735±0.0380	0.0381±0.0575	0.0646±0.0341	0.0353
NH_4^+	0.6514±0.7511	0.1512±0.0880	0.0776±0.0380	0.1276±0.0578	0.0813±0.0340	0.2178
Na^+	0.2983±0.5831	0.0806±0.0686	0.1095±0.0302	0.0595±0.0451	0.0504±0.0266	0.1196
K^+	0.3371±0.5843	0.1986±0.0697	0.3328±0.0343	0.2308±0.0466	0.2141±0.0286	0.2627
OC1	0.0000±4.0102	0.0000±0.4726	0.0000±0.2042	0.0000±0.3104	0.0222±0.1826	0.0044
OC2	0.0000±4.0745	0.2442±0.4819	0.0220±0.2078	0.0541±0.3159	0.1218±0.1864	0.0884
OC3	2.3765±5.0110	0.7879±0.6014	0.1151±0.2525	1.5674±0.4519	0.5014±0.2371	1.0697
OC4	1.4359±4.1390	0.9913±0.4981	0.2780±0.2119	0.9295±0.3301	0.3969±0.1915	0.8063
OP	0.0959±4.0620	1.2903±0.5229	0.2069±0.2098	1.5777±0.3804	0.4659±0.1972	0.7273
OC	3.9083±9.5733	3.3137±1.1616	0.6221±0.4878	4.1287±0.8149	1.5081±0.4489	2.6961
EC1	0.0385±1.1067	0.9678±0.2247	0.1546±0.0622	1.1654±0.2039	0.3467±0.0787	0.5346
EC2	0.0483±1.1899	0.3225±0.1412	0.0761±0.0607	0.4129±0.0941	0.1243±0.0545	0.1968
EC3	0.3762±0.9884	0.0807±0.1200	0.0154±0.0501	0.0682±0.0785	0.0298±0.0455	0.1141
EC	0.3671±4.4853	0.0807±0.5954	0.0392±0.2324	0.0687±0.4445	0.0349±0.2230	0.1181
TC	4.2754±10.5764	3.3944±1.3055	0.6612±0.5403	4.1974±0.9284	1.5430±0.5013	2.8143
CO_3-C	2.2379±0.9875	3.2975±0.2607	2.6516±0.1602	1.4465±0.1125	1.0376±0.0757	2.1342

leaching can decrease the CO_3-C content (Wen, 1989; Cao et al., 2005). Carbonate can also be formed in fine particles like $PM_{2.5}$ and PM_1 (Wen, 1989), which may result in the high variability of Ca contents. The abundance of Fe was lower in $PM_{2.5}$ than PM_1. The major mineral forms of Fe in loess are magnetite (Fe_3O_4), hematite (Fe_2O_3), and goethite [FeO(OH); Liu, 1985]. The abundance of K is similar (2–3%) in four fractions.

Other trace elements detected varied from 0.0001% to <1%. The clay and heavy minerals reflect the wide ranges and phases in loess sediments (Wen, 1989). Trace elements with abundances between 0.1% and 1% included Na (~0–1.7%), Mg (~0.1–0.6%), Ti (0.3–0.5%), and Mn (0.06–0.15%). Na can be influenced by chemical leaching as well as anthropogenic sources, resulting in high variability in four fractions at five sites. Mg, Ti, and Mn are crustal elements with inertial chemical reactivity, so the abundances were relatively stable in different sizes and locations. Trace elements with abundances between 0.01% and 0.1% included P, S, Cl, V, Cr, Co, Zn, Rb, Sr, Zr, and Ba. These elements were relatively higher in the PM_{10}, $PM_{2.5}$, and PM_1 size fractions, which may be associated with the mineral phase of these elements in small particles (Wen, 1989). Trace elements with abundances between 0.0001% and 0.01% included Ni, Cu, Ga, As, Se, Br, Mo, Ag, Cd, Sn, Hg, and Pb. Their abundances were also lower in TSP than PM_{10}, $PM_{2.5}$, and PM_1 fractions except for Cd. Increasing abundances with decreasing particle size is most apparent for As, where abundances in PM_{10}, $PM_{2.5}$, and PM_1 are two, three, and six-fold those found in TSP, respectively. The abundances of eight rare elements, including Y, Pd, In, Sb, La, Au, Tl, and U, were less than 0.01%, most of them close to the detection limits of XRF.

3.1.2. Water-soluble ions compositions

Among the six ions (Cl^-, NO_3^-, SO_4^{2-}, NH_4^+, Na^+, and K^+) measured, Cl^-, NH_4^+, and K^+ were abundant with the least abundance found in NO_3^-. The abundances of Cl^-, NH_4^+, Na^+, and K^+ are relatively lower in TSP than other size fractions. Abnormally high K^+ in these profiles may be ascribed to the deposition of potassic particles originated from rural biomass burning and the usage of potassic fertilizer. Elevated NH_4^+ may also be attributed to extensive fertilization during agricultural operation in the Loess Plateau. High Cl^- and Na^+ may be associated with the deposition of eolian dust originated from salt deposits in upwind regions like Qaidam salt lake (Wen, 1989). Low SO_4^{2-} abundances (0.0353–0.0565%) reflect the negligible background contents in natural loess soil and low SO_4^{2-} deposition the SO_2-containing industrial plume in the plateau.

3.1.3. Carbon fractions

Carbon is a major chemical component in polluted atmospheres, especially in $PM_{2.5}$ and PM_1 (e.g., Watson and Chow, 2002; Cao et al., 2003a, 2005, 2007; Chow et al., 2005; Chow and Watson, 2007). Carbon fraction can be classified into OC, EC, and CO_3-C (Wolff, 1968). OC abundances were around 1–3% in the four size fractions, consistent with reported OC levels in loess sediments (Wen, 1989). OC accounts for 90% of total carbon ($TC = OC + EC + CO_3$-C) in all profiles except for the $PM_{2.5}$ sample taken at the Yulin site. OC content is associated with agriculture and biological activities in the surface soil of the Loess Plateau. EC was low, in the range 0.01–0.5%, consistent with those found in the surface soil (Han et al., 2007). EC in loess originates from the deposition of anthropogenic combustion particles. Most of EC is associated with submicron particles (Seinfeld and Pandis, 1998), therefore, the EC loading in PM_1 profiles are more than one order of magnitude higher than those found in TSP or PM_{10} (Tables 2–5). All the OC/EC ratios in the four size fractions were >10.0 except for the $PM_{2.5}$ sample collected at the Yulin site. These results are similar to the soil profile findings in California's Imperial Valley (EC = 0.3–3.37%), the Mexicali road dust profile (EC = 1.06%) (Watson and Chow, 2001), and fugitive dust for $PM_{2.5}$ in Hong Kong (EC = 0.66–3.84%) (Ho et al., 2003). Crop debris, burn residue, and agricultural chemicals (e.g. pesticides, herbicides, fertilizers) in the Loess Plateau might enhance the OC abundance relative to EC.

CO_3-C accounted for about 1–5% of PM mass, similar to OC, but had low concentrations in TSP compared to other size fractions. The CO_3-C exhibited similar variations to Ca, confirming the dominance of calcite in loess. The ratios of Ca/CO_3-C ranged from 2.9 to 4.8 (average 3.9) in TSP, from 2.1 to 3.9 (average 3.2) in PM_{10}, from 2.7 to 7.5 (average 4.8) in $PM_{2.5}$, and from 3.8 to 7.4 (average 5.0) in PM_1. Most of these ratios were similar to the Ca/CO_3-C ratio of 3.3 for calcite.

3.1.4. Source characterization of composite profiles in the Chinese Loess Plateau

Composite source profiles were derived for each size fraction by averaging the profiles from the five sites. Fig. 2 shows the composite profile for each size fractions. There is no apparent difference among the four composite profiles, suggesting the chemical uniformity of loess materials (Liu, 1985; Wen, 1989). Most of the maximum-to-minimum (max/min) ratios were less than 5.0 for the 58 reported species except for As (6.8), Cd (14.9), La (8.7), Au (53), U (19), OC1 (7.1), EC3 (7.1), and EC (6.2). The abundances of major species (>1%) include Al, Si, K, Ca, Fe, OC, and CO_3-C. The levels of the major elements Al, K, Ca, and Fe in TSP were close to the concentration of bulk loess samples (Wen, 1989) (Table 2). Si in TSP (18%) is 30% lower than those in loess samples (~25%). The levels of trace elements (Ti, Mn, V, Cr, Co, Ni, Cu, Zn, Ga, As, Sr, Zr, Ba, and Se) in TSP are also close to their concentrations in loess samples (Table 2). Loess Plateau is a large-scale receptor region of eolian dust from northwest China and central Asia. Long-range transport of eolian dust makes loess deposit highly uniform (Wen, 1989). So the composite profiles can be used as fingerprints to trace Asian dust.

Even though most species had similar abundances in composite profiles, different abundances were found for some elements in different size-differentiated profiles. For example, the abundances of Al were ~5.6%, 9.1%, 4.5%, and 4.9% in TSP, PM_{10}, $PM_{2.5}$, and PM_1 fractions, respectively (Fig. 2). Past studies used the average contents of Al in bulk loess (8%) or upper continental crust (UCC; 6%) to estimate the amount of Asian dust (Zhang et al., 1997; Gao et al., 1997; Arimoto et al., 2004). This study demonstrated that size-fractionated Al varied by two-fold among the four size fractions; therefore, it is important to use size-differentiated Al abundances to calculate Asian dust.

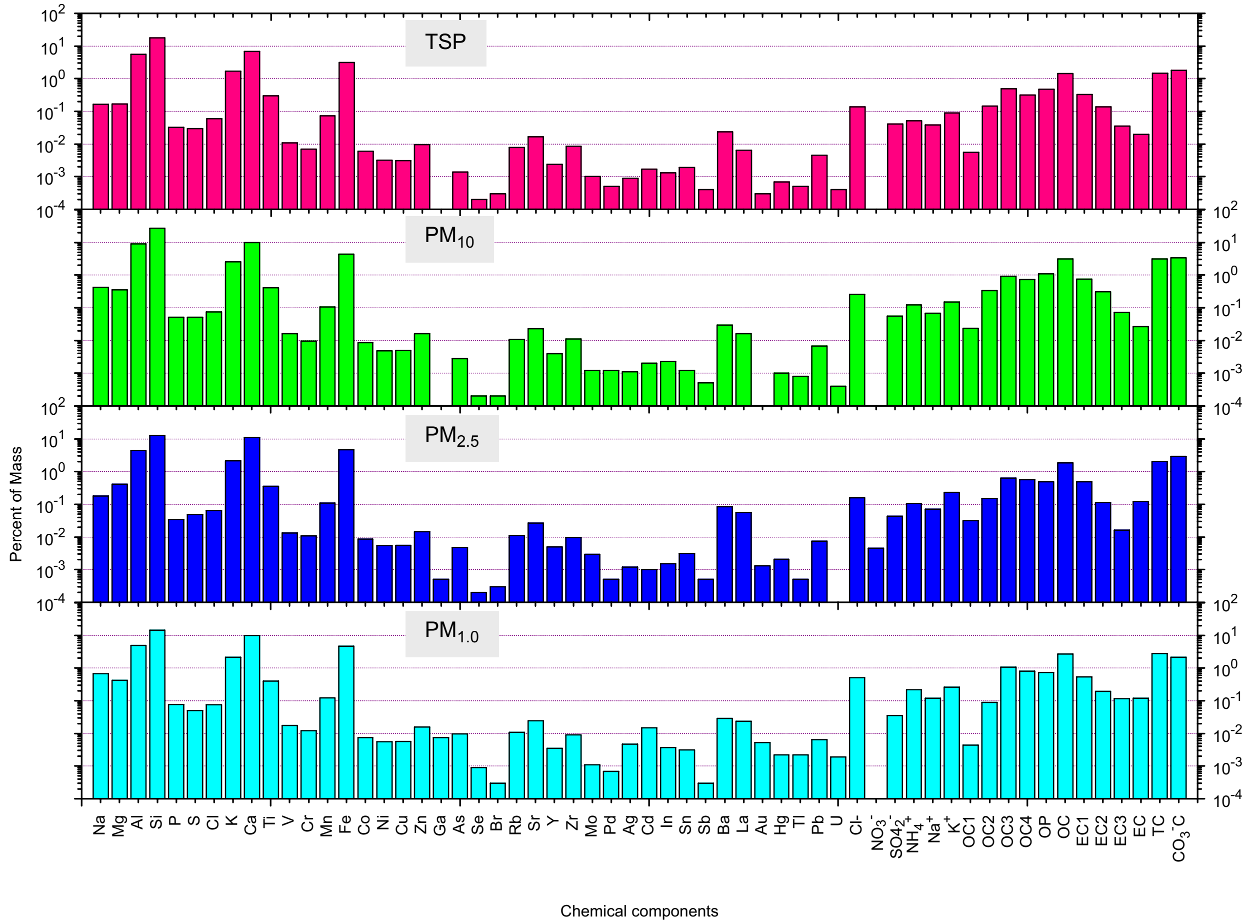

Fig. 2. Chemical components for composite profiles of TSP, PM_{10}, $PM_{2.5}$, and PM_1.

3.2. Comparison to upper continental crust (UCC)

A comparison between the observed elemental abundances in the soil sample and the composition of the Earth's UCC was made to determine the magnitude and patterns of soil enrichments. Enrichment factors (EFs), calculated relative to the composition of the UCC, have been commonly used in aerosol studies (Cao et al., 2003b; Zhang et al., 2005). This is a simple, semi-quantitative way of determining whether the elemental concentrations in the samples of interest are consistent with or enriched relative to what one would expect from the amount of crustal/mineral matter in the sample. EFs were calculated by

$$\mathrm{EF}_{\mathrm{crust}} = (X/\mathrm{Al})_{\mathrm{samples}}/(X/\mathrm{Al})_{\mathrm{crust}}, \quad (1)$$

where X refers to the concentration of the element of interest and reference element refers to the concentration of crustal rock, most commonly Al or Si. Al is used as the reference element in this paper, and the compilation of Taylor and Malennan (1995) for $(X/\mathrm{Al})_{\mathrm{crust}}$ is used to calculate EFs.

If EF approaches unity, crustal material is probably the predominant source for element X. Fig. 3 shows that there is no large difference between EFs for most elements among the four fractions. The EFs were in the range of 1–10 for the 18 crustal-related elements (Na, Mg, Si, K, Ca, Ti, V, Cr, Mn, Fe, Ni, Cu, Zn, Rb, Sr, Y, Zr, Ba). The ratios of these elements to Al can be used as fingerprints to trace the transport of Asian dust (Zhang et al., 1997; Gao et al., 1997; Arimoto, et al., 2004; Shen et al., 2007). Compared to the crustal-derived elements, the EFs for Co, As, Se, Mo, Cd, In, Sb, and Tl are one to two orders of magnitude higher, suggesting the influence of anthropogenic pollution sources. EFs of Sn, La, Pb, U exceeded 10 in some profiles, implying the impacts of non-crustal sources. Chinese Loess Plateau is an agricultural base, with almost no major industries inside. Wen (1989) showed that elevated Co and Mo concentrations originated from the usage of inorganic fertilizers. Coal and biofuel are the dominant energy sources for residents of the Plateau, so the combustion-related particles in surface soil contain toxic elements such as As, Se, Sb, and Tl. With the implementation of Western Development in China, emissions from large industrial factories like chemical plants, refined coal plants in the Ningxia and Shaanxi Provinces may increase the abundances of pollution-derived elements such as Cd, In, Sn, and Pb.

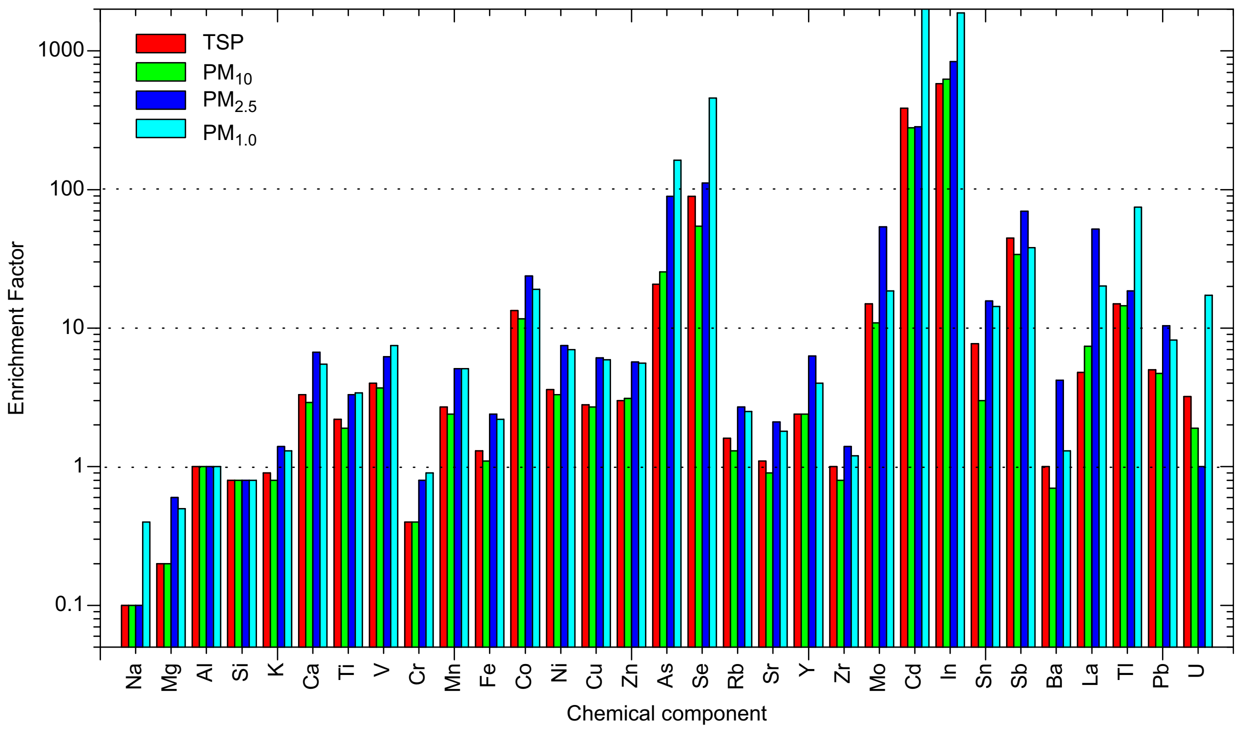

Fig. 3. Elemental enrichment factors relative to UCC (upper continental crust, Taylor and Malennan, 1995) for TSP, PM_{10}, $PM_{2.5}$, and PM_1 of composite profiles. Al is used as reference element.

3.3. Comparison with aerosol observation

Limited aerosol observations were reported for the Asian dust source regions. $PM_{2.5}$ data from Zhenbeitai, Yulin (Arimoto et al., 2006), which is located near the Mu Us Desert, a major source of Asian dust, are used for comparison. Fig. 4 shows that EFs for crustal elements, including Si, K, Ca, Ti, Mn, Fe, Sr, and Ba, are found on or below the 1:1 line, implying similar source impacts between loess and aerosol samples. However, most of the pollution elements showed enrichment in the ambient samples. For the aerosol samples, Co, Mo, Ag, Cd, and Hg are depleted but pollution-derived V, Cr, Ni, Cu, Zn, Sb, and Pb are enriched, i.e., two to three times more abundant than those found in loess samples (Fig. 4). This implies Asian dust contains pollution elements even in the close downwind regions of desert in northwest China. Since SO_4^{2-} and NO_3^- have low abundances in $PM_{2.5}$ loess samples (Table 4), the high enrichments (230-fold for SO_4^{2-}, 480-fold for NO_3^-) in aerosol samples (Fig. 4) suggested the secondary nature of these ionic species and their impact from distant anthropogenic pollution sources. Transported Asian dust is contaminated with polluted aerosol. The phenomenon was also observed by Erel et al. (2006) in desert dust over the Eastern Mediterranean region.

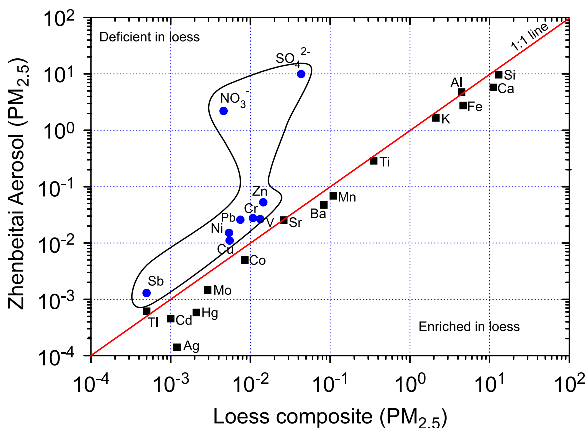

Fig. 4. Comparison of $PM_{2.5}$ chemical components between aerosol and composite loess samples from Zhengbeitai, Yulin, China. Axes are these mass fractions in the samples. The encircled components demonstrate an enrichment in ambient $PM_{2.5}$ with respect to the loess composition.

3.4. Comparison of dust characterization with other studies

Most of the past studies used elemental ratios as characteristics of Asian dust or source tracers (Arimoto et al., 2006). For example, VanCuren and Cahill (2002) used Al/Ca and K/Fe ratios to distinguish Asian from African dust. Table 6 summarizes the elemental ratios of Si, K, Ca, Ti, Mn, and Fe to Al in China along with the downwind regions of Korea, Japan, and the North Pacific. The elemental ratios of African dust were also used for comparison. The Si/Al ratios (~7.7) in China's Desert and Gobi soil (<100 μm) are two to three times higher than those reported in this study. This may be due to the differences in particle sizes, i.e., the Si content was enriched in large particles with 10–100 μm diameters. The K/Al (0.4), Ti/Al (0.08), Mn/Al (0.016), and Fe/Al (0.71) ratios over the North Pacific remain similar to the four size-fractionated composite profiles in this study, implying these crustal elements conserve the elemental signatures of Asian dust during long-range transport.

The Ca/Al ratio varied from 1.08 to 2.70 over Chinese Loess Plateau, from 0.35 to 1.60 over downwind regions in China (Beijing, Qingdao), from 0.56 to 1.14 in Korea (Seoul, Gwang Ju, Gosan), from 0.13 to 0.71 in Japan (Yaku, Nagaya, Tsukuba, Naha, and Fukuoka), and was highest (1.31) over the North Pacific. The relative enrichment of Ca in Asian dust results in the high Ca/Al ratios of dust aerosol over source and downwind regions. For example, high carbonate associated with Ca was observed in dust storm atmosphere in Xi'an (Cao et al., 2005). This distinguish feature of high Ca contents was also demonstrated by several previous studies (Wang et al., 2005; Arimoto et al., 2006). The high alkaline nature of Asian dust not only minimizes ocean acidification in the North Pacific by "alkaline pump" but also counteracts the acid rain by "rain pump" in Asia-Pacific regions (Cao et al., 2005). The Ca/Al ratios in source regions of Asian dust (0.74–2.7) are one order of magnitude higher than those in African dust (0.15–0.38). The enrichment of Ca in Asian dust lead to the high values of Ca/Al, Ca/Si, and Ca/Fe (Table 6) which are considered as source signatures to distinguish Asian versus African dust (Arimoto et al., 2006). The lower ratios of Ca/Al in Qingdao, China (0.35), Gosan (0.56), and four cities in Japan (0.15–0.24) are likely due to the reaction between

Table 6
Comparison of elemental ratios for dust events observed in Northeastern Asia and other regions

Region	Site	Size	Sample type	Si/Al	K/Al	Ca/Al	Ti/Al	Mn/Al	Fe/Al	Si/Ca	Si/Fe	Fe/Ca	K/Fe	Source of data
China	Chinese Loess Plateau	TSP	Source	3.14	0.31	1.22	0.053	0.013	0.56	2.59	5.62	0.46	0.55	This study
	Chinese Loess Plateau	PM_{10}	Source	3.00	0.28	1.08	0.045	0.012	0.48	2.79	6.24	0.45	0.57	This study
	Chinese Loess Plateau	$PM_{2.5}$	Source	2.90	0.47	2.50	0.079	0.025	1.05	1.16	2.77	0.42	0.45	This study
	Chinese Loess Plateau	PM_1	Source	2.91	0.44	2.04	0.081	0.025	0.96	1.43	3.02	0.47	0.46	This study
	Chinese Loess Plateau	TSP	Ambient	2.50	0.95	2.70	0.14		0.77	0.93	3.25	0.29	1.23	Zhang et al. (2001)
	Chinese desert regions	TSP	Ambient	3.90	0.47	1.90	0.12		0.82	2.05	4.76	0.43	0.57	Zhang et al. (2001)
	Desert soil	$<100\,\mu m$	Source	7.68	0.34	0.94	0.058	0.010	0.54	8.15	14.34	0.57	0.64	Ta et al. (2003)
	Gobi Soil	$<100\,\mu m$	Source	7.85	0.39	1.17	0.041	0.009	0.35	6.69	22.21	0.30	1.10	Ta et al. (2003)
	Dust storm over NW China	TSP	Ambient	2.94	0.27	0.74	0.031	0.008	0.35	3.98	8.49	0.47	0.78	Ta et al. (2003)
	Yulin, China	PM_9	Ambient	2.79	0.31	0.79	0.054	0.015	0.63	3.53	4.43	0.80	0.49	Alfaro et al. (2003)
	Yulin, China	$PM_{2.5}$	Ambient		0.46	0.81	0.072	0.023	0.51			0.63	0.90	Xu et al. (2004)
	Yulin, China	$PM_{2.5}$	Ambient	1.90	0.52	1.00	0.051	0.015	0.59	1.90	3.22	0.59	0.88	Arimoto et al. (2004)
	Beijing, China	$PM_{2.5}$	Ambient			1.60	0.064	0.011	0.67			0.42		Sun et al. (2004)
	Qingdao, China	$PM_{2.5}$	Ambient			0.35	0.058	0.018	0.61			1.75		Guo et al. (2004)
Korea	Seoul, South Korea	PM_{10}	Ambient			0.66		0.015	0.61		0.00	0.93	0.00	Choi et al. (2001)
	Seoul. South Korea	PM_{10}	Ambient		0.36	0.83	0.047	0.033	0.83		0.00	1.00	0.43	Kim et al. (2003)
	Seoul. South Korea	$PM_{2.5}$	Ambient		0.45	0.74	0.043	0.040	0.87		0.00	1.17	0.52	Kim et al. (2003)
	Gwang Ju, South Korea	$PM_{2.5}$	Ambient		0.52	0.64	0.028	0.025	0.67			1.05	0.77	Kim et al. (2003)
	Gosan, South Korea	TSP	Ambient			1.14	0.037	0.027	1.21		0.00	1.06	0.00	Park et al. (2003)
	Gosan, South Korea	TSP	Ambient	1.44	0.28	0.56	0.050		0.48	2.57	3.00	0.86	0.58	Arimoto et al. (2006)
Japan	Yaku shima, Japan	TSP	Ambient		0.37	0.71		0.014	0.52			0.73	0.71	Nishikawa et al. (1991)
	Nagoya, Japan	PM_{11}	Ambient		0.18	0.16	0.053	0.009	0.49			3.18	0.37	Ohta et al. (2003)
	Tsukuba, Japan	PM_{11}	Ambient		0.29	0.13	0.056	0.008	0.52			3.97	0.55	Ohta et al. (2003)
	Naha, Japan	PM_{11}	Ambient		0.22	0.24	0.051	0.008	0.53			2.16	0.43	Ohta et al. (2003)
	Fukuoka, Japan	PM_{11}	Ambient		0.29	0.15	0.046	0.011	0.50			3.34	0.58	Ohta et al. (2003)
Others	North Pacific	TSP	Ambient		0.40	1.31	0.080	0.016	0.71			0.54	0.57	Holmes and Zoller (1996)
	African Dust (Eastern US)	TSP	Ambient	1.84		0.15			0.47	12.27	3.91	3.13		Perry et al. (1997)
	African Dust (Puerto Rico)	TSP	Ambient	2.12	0.17	0.38	0.05		0.30	5.58	7.07	0.79	0.57	Reid et al. (2003)
	Upper Continental Crust			3.83	0.35	0.37	0.037	0.007	0.44	10.27	8.81	1.17	0.80	Taylor and Malennan (1995)

dust and the polluted aerosols and the depletion of Ca during long-range transport under low dust layer (Arimoto et al., 2006).

4. Conclusions

Characteristics for TSP, PM_{10}, $PM_{2.5}$, and PM_1 of loess samples in Chinese Loess Plateau are examined. A total of 60 source profiles were developed for 15 samples acquired at three loess zones in the middle reaches of the Yellow River Valley. Chemical species with abundances $>1\%$ included Al, Si, K, Ca, Fe, OC and CO_3-C, in four size-differentiated source profiles. OC accounted for $\sim90\%$ of total carbon in most of the profiles with negligible amounts of EC. EFs indicated that 18 elements (Na, Mg, Si, K, Ca, Ti, V, Cr, Mn, Fe, Ni, Cu, Zn, Rb, Sr, Y, Zr, and Ba) in the samples were dominated by crustal sources and eight elements (Co, As, Se, Mo, Cd, In, Sb, and Tl) were influenced by anthropogenic pollution sources. Compared to loess profiles, $PM_{2.5}$ Zn, Cr, V, Ni, Pb, Cu, Sb, SO_4^{2-}, and NO_3^- were enriched in ambient samples acquired from nearby downwind regions, which implies Asian dust contained pollution components. The elemental ratios of Si, K, Ca, Ti, Mn, and Fe to Al in source regions of Asian dust in China compared well with those found at downwind regions like Korea, Japan, and the North Pacific. The enrichment of Ca in Asian dust lead to the high values of Ca/Al, Ca/Si, and Ca/Fe which are considered as source signatures to distinguish Asian dust from other regions like African dust. Detailed chemical characteristics for different size fractions of loess samples can be severed as natural background information of Asian dust and as a basic database of fugitive dust for PM source apportionment, which also can benefit research on the modern dust and paleoclimate evolutions.

Acknowledgments

We are grateful to all the technical staff at Environmental Analysis Facility (EAF) at the Desert Research Institute (DRI), Reno, NV, for their assistance in analytical work. The authors wish to thank Jo Gerrard for editing the manuscript. This work was financially supported by Grants from a National Key Project of Basic Research (2004CB720203), and the Chinese National Science Foundation (40121303, 40675081).

References

Alfaro, S.C., Gomes, L., Rajot, J.L., Lafon, S., Gaudichet, A., Chatenet, B., Maille, M., Cautenet, G., Lasserre, F., Cachier, H., 2003. Chemical and optical characterization of aerosols measured in spring 2002 at the ACE-Asia supersite, Zhenbeitai, China. Journal of Geophysical Research 108 (D23), 8641.

An, Z.S., Kukla, G., Porter, S.C., 1990. Late quaternary dust flow on the Chinese Loess Plateau. Quaternary International 18, 125–132.

Arimoto, R., Zhang, X.Y., Huebert, B.J., Kang, C.H., Savoie, D.L., Prospero, J.M., Sage, S.K., Schloesslin, C.A., Khaing, H.M., Oh, S.N., 2004. Chemical composition of atmospheric aerosols from Zhenbeitai, China, and Gosan, South Korea, during ACE-Asia. Journal of Geophysical Research 109 (D19S04).

Arimoto, R., Kim, Y.J., Kim, Y.P., Quinn, P.K., Bates, T.S., Anderson, T.L., Gong, S., Uno, I., Chin, M., Huebert, B.J., Clarke, A.D., Shinozuka, Y., Weber, R.J., Anderson, J.R., Guazzotti, S.A., Sullivan, R.C., Sodeman, D.A., Prather, K.A., Sokolik, I.N., 2006. Characterization of Asian dust during ACE-Asia. Global and Planetary Change 52, 23–56.

Ashbaugh, L.L., Carvacho, O.F., Brown, M.S., Chow, J.C., Watson, J.G., Magliano, K.C., 2003. Soil sample collection and analysis for the fugitive dust characterization study. Atmospheric Environment 37, 1163–1173.

Biscaye, P.E., Grousset, F.E., Revel, M., Van der Gaast, S., Zielinski, G.A., Vaars, A., Kukla, G., 1997. Asian provenance of last glacial maximum dust in GISP2 ice core, summit, Greenland. Journal of Geophysical Research 102, 26765–26781.

Cao, J.J., Lee, S.C., Ho, K.F., Zhang, X.Y., Zou, S.C., Fung, K., Watson, J.G., Chow, J.C., 2003a. Characteristics of carbonaceous aerosol in Pearl river delta region, China during 2001 winter period. Atmospheric Environment 37, 1451–1460.

Cao, J.J., Lee, S.C., Zheng, X.D., Ho, K.F., Zhang, X.Y., Guo, H., Chow, J.C., Wang, H.B., 2003b. Characterization of dust storms to Hong Kong in April 1998. Water, Air, and Soil Pollution: Focus 3, 213–229.

Cao, J.J., Lee, S.C., Zhang, X.Y., Chow, J.C., An, Z.S., Ho, K.F., Watson, J.G., Fung, K., Wang, Y.Q., Shen, Z.X., 2005. Characterization of airborne carbonate over a site on Asian dust source regions during spring 2002 and its climatic and environmental significance. Journal of Geophysical Research 110 (D03203).

Cao, J.J., Lee, S.C., Chow, J.C., Watson, J.G., Ho, K.F., Zhang, R.J., Jin, Z.D., Shen, Z.X., Chen, G.C., Kang, Y.M., Zou, S.C., Zhang, L.Z., Qi, S.H., Dai, M.H., Cheng, Y., Hu, K., 2007. Spatial and seasonal distributions of carbonaceous aerosols over China. Journal of Geophysical Research 112 (D22S11), 1–9.

Choi, J.C., Lee, M., Chun, Y., Kim, J., Oh, S., 2001. Chemical composition and source signature of spring aerosol in Seoul Korea. Journal of Geophysical Research 106 (D16), 18067–18074.

Chow, J.C., 1995. Measurement methods to determine compliance with ambient air quality standards for suspended particles. Journal of Air & Waste Management Association 45 (5), 320–382.

Chow, J.C., Watson, J.G., 1998. Guideline on speciated particulate monitoring. Third Draft Report. Prepared for

US Environmental Protection Agency, Office of Air Quality Planning and Standards, Research Triangle Park, NC, by Desert Research Institute, Reno, NV, August 1998. 〈http://www.epa.gov/ttnamti1/files/ambient/pm25/spec/drispec.pdf〉.

Chow, J.C., Watson, J.G., 1999. Ion chromatography in elemental analysis of airborne particles. In: Landsberger, S., Creatchman, M. (Eds.), Elemental Analysis of Airborne Particles. Gordon and Breach Publishers, New York, NJ, pp. 539–573.

Chow, J.C., Watson, J.G., 2007. Survey of measurement and composition of ultrafine particles. Aerosol and Air Quality Research 7 (2), 121–173.

Chow, J.C., Watson, J.G., Pritchett, L.C., Pierson, W.R., Frazier, C.A., Purcell, R.G., 1993. The DRI thermal/optical reflectance carbon analysis system: description evaluation and applications in US air quality studies. Atmospheric Environment 27, 1185–1201.

Chow, J.C., Watson, J.G., Houck, J.E., Pritchett, L.C., Rogers, C.F., Frazier, C.A., Egami, R.T., Ball, B.M., 1994. A laboratory resuspension chamber to measure fugitive dust size distribution and chemical composition. Atmospheric Environment 28, 3463–3481.

Chow, J.C., Watson, J.G., Crow, D., Lowenthal, D.H., Merrifield, T., 2001. Comparison of IMPROVE and NIOSH carbon measurements. Aerosol Science and Technology 34, 23–24.

Chow, J.C., Watson, J.G., Kuhns, H.D., Etyemezian, V., Lowenthal, D.H., Crow, D.J., Kohl, S.D., Engelbrecht, J.P., Green, M.C., 2004. Source profiles for industrial, mobile, and area sources in the big bend regional aerosol visibility and observational (BRAVO) study. Chemosphere 54 (2), 185–208.

Chow, J.C., Watson, J.G., Chen, L.-W.A., Paredes-Miranda, G., Chang, M.-C.O., Trimble, D., Fung, K.K., Zhang, H., Yu, J.Z., 2005. Refining temperature measures in thermal/optical carbon analysis. Atmospheric Chemistry and Physics 5 (4), 2961–2972.

Chow, J.C., Watson, J.G., Chen, L.-W.A., Chang, M.-C.O., Robinson, N.F., Trimble, D.L., Kohl, S.D., 2007. The IMPROVE_A temperature protocol for thermal/optical carbon analysis: maintaining consistency with a long-term data base. Journal of Air & Waste Management Association 57, 1014–1023.

Duce, R.A., Unni, C.K., Ray, B.J., Prospero, J.M., Merrill, J.T., 1980. Long range transport of soil dust from Asia to the tropical North Pacific. Science 209, 1522–1524.

Erel, Y., Dayan, U., Rabi, R., et al., 2006. Trans boundary transport of pollutants by atmospheric mineral dust. Environmental Science & Technology 40, 2996–3005.

Gao, Y., Arimoto, R., Duce, R.A., Zhang, X.Y., Zhang, G.Y., An, Z.S., Chen, L.Q., Zhous, M.Y., Gu, D.Y., 1997. Temporal and spatial distributions of dust and its deposition to the China Sea. Tellus 49B, 172–189.

Guo, Z.G., Feng, J.L., Fang, M., Chen, H.Y., Lau, K.H., 2004. The elemental and organic characteristics of $PM_{2.5}$ in Asian dust episodes in Qingdao China 2002. Atmospheric Environment 38, 909–919.

Han, Y.M., Cao, J.J., Chow, J.C., Watson, J.G., An, Z.S., Jin, Z.D., Fung, K., Liu, S.X., 2007. Evaluation of the thermal/optical reflectance method for discrimination between soot- and char-EC. Chemosphere 69, 569–574.

Ho, K.F., Lee, S.C., Chow, J.C., Watson, J.G., 2003. Characterization of PM_{10} and $PM_{2.5}$ source profiles for fugitive dust in Hong Kong. Atmospheric Environment 37, 1023–1032.

Holmes, J., Zoller, W., 1996. The elemental signature of transported Asian dust at Mauna Loa observatory. Tellus 48B, 83–92.

Kim, K.H., Choi, G.H., Kang, C.H., Lee, J.H., Kim, J.Y., Youn, Y.H., 2003. The chemical composition of fine and coarse particles in relation with the Asian dust events. Atmospheric Environment 37, 753–765.

Liu, T.S., 1985. Loess and the Environment. China Ocean Press, Beijing, pp. 1–251.

Nishikawa, M., Kanamori, S., Kanamori, N., Mizoguchi, T., 1991. Kosa aerosol as eolian carrier of anthropogenic material. Science of the Total Environment 107, 13–27.

Nishikawa, M., Quan, H., Morita, M., 2000. Preparation and evaluation of certified reference materials for Asian mineral dust. Global Environment Research 4, 103–113.

Ohta, A., Terashima, S., Kanai, Y., Kamioka, H., Imai, N., Matsuhisa, Y., Shimizu, H., Takahashi, Y., Kai, K.J., Hayashi, M., Zhang, R.J., 2003. Grain-size distribution and chemical composition of water-insoluble components in aeolian dust collected in Japan in spring 2002. Bulletin of the Geological Survey of Japan 54, 303–322.

Park, M.H., Kim, Y.P., Kang, C.H., 2003. Aerosol composition change due to dust storm: measurements between 1992 and 1999 at Gosan Korea. Water, Air, and Soil Pollution: Focus 3, 117–128.

Perry, K.D., Cahill, T.A., Eldred, R.A., Dutcher, D.D., Gill, T.E., 1997. Long-range transport of North African dust to the eastern United States. Journal of Geophysical Research 102 (D10), 11225–11238.

Reid, E.A., Reid, J.S., Meier, M.M., Dunlap, M.R., Cliff, S.S., Broumas, A., Perry, K., Maring, H., 2003. Characterization of African dust transported to Puerto Rico by individual particle and size segregated bulk analysis. Journal of Geophysical Research 108 (D19), 8591.

Seinfeld, J.H., Pandis, S.N., 1998. Atmospheric Chemistry and Physics: From Air Pollution to Climatic Change. Wiley, New York, pp. 700–709.

Shen, Z.X., Cao, J.J., Arimoto, R., Zhang, R.J., Jie, D.M., Liu, S.X., Zhu, C.S., 2007. Chemical composition and source characterization of spring aerosol over Horqin sand-land in Northeastern China. Journal of Geophysical Research—Atmospheres 112 (D14315).

Sun, Y.L., Zhuang, G.S., Yuan, H., Zhang, X.Y., Guo, J.H., 2004. Characteristics and sources of 2002 super dust storm in Beijing. Chinese Science Bulletin 49, 698–705.

Ta, W.Q., Zheng, X., Qu, J.J., Yang, G.S., Wang, T., 2003. Characteristics of dust particles from the desert/Gobi area of northwestern China during dust-storm periods. Environmental Geology 43, 667–679.

Taylor, S.R., Malennan, S.M., 1995. The geochemical evolution of the continental crust. Reviews of Geophysics 33, 241–265.

VanCuren, R.A., Cahill, T.A., 2002. Asian aerosols in North America: frequency and concentration of fine dust. Journal of Geophysical Research 107 (D24), 4804.

Vega, E., Mugica, V., Reyes, E., Sanchez, G., Chow, J.C., Watson, J.G., 2001. Chemical composition of fugitive dust emitters in Mexico city. Atmospheric Environment 35, 4033–4039.

Wang, Y.Q., Zhang, X.Y., Arimoto, R., Cao, J.J., Shen, Z.X., 2005. Characteristics of carbonate content and carbon and oxygen isotopic composition of northern China soil and dust aerosol and its application to tracing dust sources. Atmospheric Environment 39, 2631–2642.

Watson, J.G., Chow, J.C., 2001. Source characterization of major emission sources in the Imperial and Mexicali valleys along the US Mexico border. Science of the Total Environment 276, 33–47.

Watson, J.G., Chow, J.C., 2002. Comparison and evaluation of in-situ and filter carbon measurements at the Fresno supersite. Journal of Geophysical Research 107 (D21) ICC 3-1-ICC 3-15.

Watson, J.G., Chow, J.C., 2004. Receptor models for air quality management. Environmental Management 10, 15–24.

Watson, J.G., Chow, J.C., 2007. Receptor models for source apportionment of suspended particles. In: Murphy, B., Morrison, R. (Eds.), Introduction to Environmental Forensics, second ed. Academic Press, New York, NY, pp. 279–316.

Watson, J.G., Chow, J.C., Frazier, C.A., 1999. X-ray fluorescence analysis of ambient air samples. In: Landsberger, S., Creatchman, M. (Eds.), Elemental Analysis of Airborne Particles. Gordon and Breach Publishers, New York, NJ, pp. 67–96.

Watson, J.G., Zhu, T., Chow, J.C., Engelbrecht, J.P., Fujita, E.M., Wilson, W.E., 2002. Receptor modeling application framework for particle source apportionment. Chemosphere 49 (9), 1093–1136.

Wen, Q.Z., 1989. Chinese Loess Geochemistry. Science Press, Peking, pp. 1–285 (in Chinese).

Wolff, G.T., 1968. Particulate elemental carbon in the atmosphere. Journal of Air Pollution Control Association 31, 935–938.

Xu, J., Bergin, M.H., Greenwald, R., Schauer, J.J., Shafer, M.M., Jaffrezo, J.L., Aymoz, G., 2004. Aerosol chemical, physical, and radiative characteristics near a desert source region of northwest China during ACE-Asia. Journal of Geophysical Research 109 (D19S03).

Yuan, C.S., Hai, C.X., Zhao, M., 2006. Source profiles and fingerprints of fine and coarse sands resuspended from soils sampled in central inner Mongolia. China Particuology 4, 304–311.

Zhang, R.J., Arimoto, R., An, J.L., Yabuki, S., Sun, J., 2005. Ground observations of a strong dust storm in Beijing in March 2002. Journal of Geophysical Research 110 (D18S06).

Zhang, X.Y., Arimoto, R., An, Z.S., 1997. Dust emission from Chinese desert sources linked to variations in atmospheric circulation. Journal of Geophysical Research 102 (D23), 28041–28047.

Zhang, X.Y., Arimoto, R., Cao, J.J., An, Z.S., Wang, D., 2001. Atmospheric dust aerosol over the Tibetan plateau. Journal of Geophysical Research 106 (D16), 18471–18476.

Zhang, X.Y., Cao, J.J., Li, L.M., Arimoto, R., Cheng, Y., Huebert, B., Wang, D., 2002. Characterization of atmospheric aerosol over Xi'an in the South Margin of the Loess plateau China. Atmospheric Environment 36, 4189–4199.

Zhao, P.S., Feng, Y.C., Zhu, T., Wu, J.H., 2006. Characterizations of resuspended dust in six cities of North China. Atmospheric Environment 40, 5807–5814.